A Systematic Conformal Finite-Difference Time-Domain (FDTD) Technique for the Simulation of Arbitrarily Curved Interfaces Between Dielectrics

Theodoros I. Kosmanis, *Student Member, IEEE,* and Theodoros D. Tsiboukis, *Senior Member, IEEE*

***Abstract*—A systematic, three-dimensional methodology is presented in this paper for the finite-difference time-domain modeling of curved dielectric interfaces. Prism cells, appropriately arranged around the interface in order to preserve the duality of the overall lattice, are utilized for the accurate geometrical representation of the arbitrarily shaped dielectrics. The new scheme is enhanced by projection coefficients for the connection of field fluxes and field intensities, and appropriately computed effective permittivity values along the interface between the two media. The minor percentage of these cells in relation to the classical ones that complete the computational grid, minimizes the algorithm's complexity and resource requirements. Its efficiency is proved via the analysis of partially filled resonant cavities.**

***Index Terms*—Finite-difference time-domain (FDTD) methods, microwave devices, resonators.**

I. Introduction

DURING the last decade, various techniques have been proposed in order to extend the applicability of the finite-difference time-domain (FDTD) method to the numerical analysis of electromagnetic devices and components consisting of irregular shapes and curved boundaries [1]. Local conformal schemes have shown considerable accuracy, demanding limited computational resources, since they discretize most of the domain of interest with the well-known Yee cells. Nevertheless, the great majority of these schemes deal with perfectly conducting materials [2]–[4], while in a small number of them dielectric interfaces are studied only in two dimensions [2]. On the other hand, although global techniques [5], [6] that deal with the overall grid in a unified way, have the capability of sufficiently modeling any kind of structure, they entail a great deal of algorithmic complexity and computational resources, and hence, they could not be characterized as "easy-to-use" tools.

Consequently, the simulation of curved dielectric interfaces (e.g., dielectric resonators, conformal microstrip filters and antennas) is obtained mainly through the original staircase FDTD algorithm. The efforts for increasing the accuracy of such problems has been focused on the introduction of effective permittivities of FDTD cells [7] or edges [8], [9] along the interface, maintaining the Cartesian structure of the grid. Nevertheless, all these approaches require, in general, very dense meshes, and thus, increased computational resources for sufficient accuracy, since they are not based on the precise geometric representation of the curved interface, but on an approximation by means of orthogonal cells.

This paper introduces an innovative conformal FDTD technique in three dimensions that, unlike the aforementioned ones, can systematically treat problems involving arbitrarily shaped interfaces between dielectric materials. According to the proposed procedure, prism cells are appropriately arranged in the area around the dielectric curve, whereas the rest of the computational domain is discretized by means of the orthogonal Yee's cells. The update of field components, located at the edges of prism cells is obtained via the time stepping of the integral form of Maxwell's equations. Appropriate projection coefficients relate the field fluxes normal to cell faces to field intensities along the edges, while special permittivity values (derived by linear interpolation) are introduced for cell faces and edges that intersect the interface. Thus, the new scheme incorporates most of conformal techniques' merits, i.e., limited programming complexity and resource requirements. Furthermore, the topological treatment described above entails no algorithmic instabilities, since it preserves the duality of the lattice and therefore, it is ideal for frequency-dependent problems, such as waveguiding and resonance, that require long time sampling.

II. Dielectric Interface Modeling in Three Dimensions

We refer to a general 3-D structure comprising two dielectric materials, of permittivities ε_1 and ε_2, respectively. The interface of the two distinct regions is arbitrary in shape, according to a function, $y = D_I(x)$, with x, y corresponding to the two dimensions of the structure's cross section, while no alteration occurs in the third dimension (z).

The accurate simulation of the structure by means of the original Yee algorithm (staircase meshing) demands a great deal of computational resources due to its orthogonal nature. On the other hand, the already existing 2-D conformal technique has important deficiencies and is not straightforwardly extendable to three dimensions.

A. The "Stair-Step" Problem

The initial conformal theory, as proposed in the two dimensions, enforces the alignment of the common edge between two adjacent orthogonal cells, with the dielectric interface that intersects them. However, inspecting a wider part of the computational space (not only the restricted area of the two cells), one

Manuscript received July 5, 2001. This work was supported in part by the Greek General Secretariat of Research and Technology under Grant 99ED325.

The authors are with the Department of Electrical and Computer Engineering, Aristotle University of Thessaloniki, Thessaloniki GR-54006, Greece (e-mail: tsibukis@auth.gr).

Publisher Item Identifier S 0018-9464(02)02430-5.

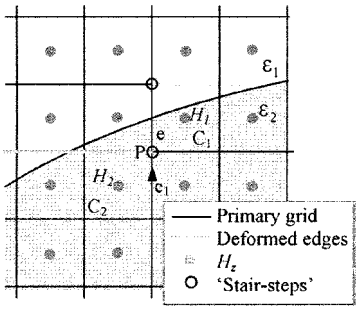

Fig. 1. The "stair-step" appears because P is a node of cell C_1, but not of the neighboring one, C_2.

can easily observe the "stair-step" problem, which arises in the primary grid when the pair of distorted cells moves a row up or down according to the curve's slope. As shown in Fig. 1, the "stair-step" is created by a cell (C_1) node (P), that does not coincide with a corresponding node of a neighboring cell (C_2), but is located along their common edge (e). This topological irregularity causes difficulty in implementing Ampere's law for the time update of the electric field component along the common edge. Therefore, it is enforced to be equal to the electric field value along the nearest edge ($e1$), since it is necessary for the time update of the magnetic intensities H_1 and H_2.

However, its extension to the three dimensions is not possible without important alterations in the lattice's structure. The local nonorthogonal structure of the primary grid and the existence of the "stair-steps" result in unorthodox complex dual grid, which is defined to have its cell vertices located at the barycenters of the primary cells. The basic topological rule that "each dual (primary) grid edge must cross only one primary (dual) grid face" is violated and therefore algorithmic instability [10]—further deteriorated by the use of the nearest neighbor extrapolation—is caused.

B. The Proposed 3-D Locally Conformal Topology

According to Section II-A, for the creation of a stable 3-D conformal FDTD algorithm, the appropriate elimination of the "stair-steps" is required. The proposed technique, overcoming any duality deficiency, is based on the discretization of the computational space near a dielectric interface, into five-faced prisms and hexahedrals (primary grid), whereas the rest of the domain maintains the orthogonal structure of the classic FDTD lattice. Complementary to the primary grid, the dual one consists of seven-faced prisms (only near the interface) and hexahedrals, leading thus, to a topologically correct scheme.

A systematic and straightforward way of forming the cells near the dielectric interface is clarified in Fig. 2, which depicts the following procedure.

1) The computational domain is discretized by means of an orthogonal classic FDTD grid.
2) The primary grid cells close to the interface are deformed in order to conform to it and better describe it. The "stair-steps," now created by cell edges not coinciding with a corresponding edge of a neighboring cell, are detected.
3) The two primary faces that are responsible for the "stair-step" formation are moved toward different directions and the corresponding cells are turned from hexahedrals into five-faced prisms (quadrilaterals into triangles in cross-section view). Therefore, the "stair-step" problem is overcome.
4) The dual grid, defined by the barycenters of the primary cells' volumes is inserted (z-directed dual edges cross the primary faces at their barycenter).

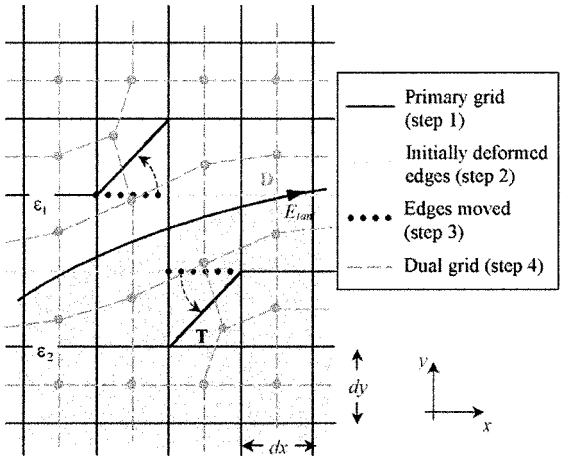

Fig. 2. Grid generation procedure and treatment of the "stair-step." For brevity the dual grid lines (half cell shifted along z-direction) are plotted on the same plane as the primary grid ones.

The mesh generation is completed by the characterization of various types of cell areas, around the curved interface, that need special treatment. Specifically, four types of cell areas in the primary grid can be distinguished according to the slope angle of the dielectric interface.

a) Region "A": Column containing one (1) five-faced prismatic cell (prism of triangular cross-section) above the dielectric interface.
b) Region "B": Column containing one (1) five-faced prismatic cell below the dielectric interface.
c) Region "AB": Column containing two (2) five-faced prismatic cells, one above and one below the dielectric interface.
d) Region "O": Column containing no five-faced prismatic cells.

It must be mentioned that a single "stair-step" is replaced via the above procedure by a pair of regions, "A" and "B." However, when the curve is very steep, $k > 1$ subsequent "stair-steps" appear in the grid, which are substituted by one region "A," $k-1$ regions "AB" and one region "B." Finally, regions "O" describe the classical, distorted, hexahedral cells in the absence of "stair-steps." Fig. 3 depicts in cross-section view the discretization of the interface between two dielectrics by the proposed method. This distinction, while requiring minor computer resources, greatly simplifies the algorithm.

The update of field components in the grid is performed by means of the integral form of Maxwell's equations, i.e., the circulation of the electric (magnetic) field along the circumference of a primary (dual) grid face is used for the update of the magnetic (electric) field normal to that face. As an example, the up-

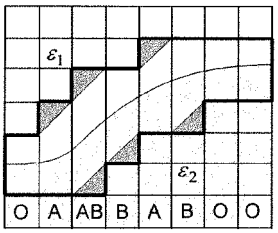

Fig. 3. The four distinct regions of the primary grid as they are formed for the simulation of an arbitrary curve. The dual grid is correspondingly created.

date of H_z located in the barycenter of triangle T and of the $E_{\tan}$ along the interface are, respectively, calculated by

$$\partial_t H_z|^n_{i,j,k} = \frac{-\delta t}{\mu_0 S_T P^h_{i,j}} \cdot \left(E_x|^n_{i,j,k}\,\delta x - E_x|^n_{i,j+1,k}\,L_T + E_y|^n_{i+1,j,k}\,\delta y \right) \quad (1)$$

and

$$\partial_t E_{\tan}|^{n+0.5}_{i,j,k} = \frac{\delta t}{\varepsilon L_D \delta z P^e_{i,j}} \cdot \begin{pmatrix} H_z|^{n+0.5}_{i,j+0.5,k}\,\delta z - H_z|^{n+0.5}_{i,j-0.5,k}\,\delta z \\ - H_y|^{n+0.5}_{i,j,k+0.5}\,L_D + H_y|^{n+0.5}_{i,j,k-0.5}\,L_D \end{pmatrix}, \quad (2)$$

where δt is the time step, δz the discretization along z direction, ε and μ_0 the permittivity and permeability appointed to the updated component, S_T the triangle area, L_D the length of dual edge D, $L_T = (\delta x^2 + \delta y^2)^{0.5}$ and $P^e_{i,j}$, $P^h_{i,j}$ the projection coefficients to be defined below.

C. Projection Coefficients

The general absence of orthogonality between the primary grid faces/edges and the dual grid edges/faces, due to the local unstructured nature of distorted cells, imposes the use of a projection scheme for the connection of the fluxes computed by Maxwell's equations to the intensities required for this computation. The formers are normal to the faces whereas the latter are aligned with the edges. Supposing that an edge intersects its dual face by an angle $\theta^{e,h}$ [Fig. 4(a)], then the following expressions relate a flux (connected to the face) to the corresponding intensity (located along the edge) and define the projection coefficients

$$\text{electric field:} \quad \overline{\mathbf{D}} = \varepsilon \overline{\mathbf{E}} \cos\theta^e \qquad P^e_{i,j} = \cos\theta^e \quad (3)$$

$$\text{magnetic field:} \quad \overline{\mathbf{B}} = \mu_0 \overline{\mathbf{H}} \cos\theta^h \qquad P^h_{i,j} = \cos\theta^h. \quad (4)$$

D. Effective Permittivities at the Dielectric Interface

When dielectric interfaces are simulated, the permittivity values appointed to the electric field components located along the interface play a very significant role. Considering the interface of Fig. 4(b), it is only the dielectric constants related to E_x and E_z along the interface that must be appropriately defined. Based on the discretization of the integral form of Maxwell's equations over finite volumes containing the interface, and the continuity conditions across it, the following effective permittivities are derived [9]:

$$\varepsilon^{eff}_{rx} = \frac{S_{ux}\delta z\varepsilon_1 + S_{dx}\delta z\varepsilon_2}{S_{ux}\delta z + S_{dx}\delta z} = \frac{S_{ux}\varepsilon_1 + S_{dx}\varepsilon_2}{S_{ux} + S_{dx}} \quad (5)$$

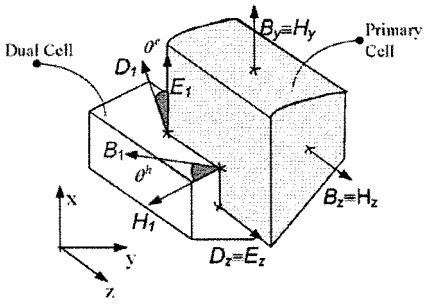

(a)

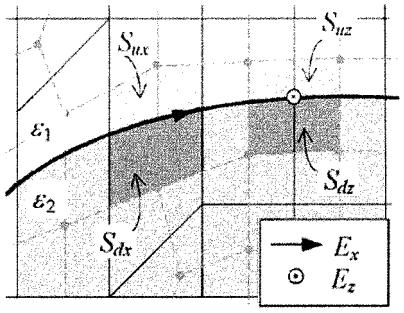

(b)

Fig. 4. (a) Field fluxes and intensities are related to each other through simple geometrical projection, (b) computation of the effective permittivities along the dielectric interface.

$$\varepsilon^{eff}_{rz} = \frac{S_{uz}\delta z\varepsilon_1 + S_{dz}\delta z\varepsilon_2}{S_{uz}\delta z + S_{dz}\delta z} = \frac{S_{uz}\varepsilon_1 + S_{dz}\varepsilon_2}{S_{uz} + S_{dz}} \quad (6)$$

where S_u and S_d are the areas of the cell belonging to the material with permittivities ε_1 and ε_2, respectively. These values, which are the outcome of linear weighting in the volume of a cell, are proved to maintain the second order accuracy of the FDTD equations.

E. Discussion

Apparently, the proposed technique preserves, in a major level, the characteristics of the classic FDTD method. Furthermore, it is advantageous over other existing conformal approaches, since it can feasibly and systematically simulate three-dimensionally curved dielectric structures, maintaining simultaneously, the duality of the grid. The avoidance of any extrapolation schemes, together with the embodying in the procedure of interpolation and projection ones, assures algorithmic accuracy and stability, as will be proved by the numerical results. Finally, the existence of deformed cells only in a three-cell width area across the modeling curve, limits the CPU and memory resources required by the new method.

The maximum value of the time step that does not lead to instability is defined by the von Neumann analysis (similar to the one of the PGY algorithm [11]) and is given by

$$\delta t \le \left[c_d \max\left\{ \sqrt{\left(\frac{1}{\delta z}\right)^2 + \left(\frac{1}{l_{k1}}\right)^2 + \left(\frac{1}{l_{k2}}\right)^2} \right\} \right]^{-1} \quad (7)$$

where c_d is the speed of light in the material with minimum permittivity and l_{k1}, l_{k2} the length of edges sharing a common vertice.

TABLE I
RESONANT FREQUENCIES ($\times 10^8$) FOR $\varepsilon_r = 38$. (A ≡ PROPOSED METHOD, B ≡ STAIRCASE FDTD METHOD, C ≡ METHOD [8])

No of cross-section cells	$q=1$			$q=2$			$q=3$		
	A	B	C	A	B	C	A	B	C
30	5.0754	4.7751	4.7425	5.2035	5.0195	4.9380	6.2015	5.8835	5.851
110	5.0395	5.043	5.075	5.3010	5.1380	5.0908	6.2250	6.0868	6.1026
440	5.059	5.059	5.091	5.3196	5.1225	5.1230	6.1884	6.1342	6.1342
990	5.075	5.075	5.085	5.3121	5.3121	5.3121	6.1660	6.1184	6.1469
1760	5.06	5.0592	5.06	5.2973	5.3121	5.3121	6.1435	6.134	6.134

TABLE II
RESONANT FREQUENCIES ($\times 10^8$) FOR $q = 2$. (A ≡ PROPOSED METHOD, B ≡ STAIRCASE FDTD METHOD, C ≡ METHOD [8])

No of cross-section cells	$\varepsilon_r = 2.495$			$\varepsilon_r = 20$			$\varepsilon_r = 38$		
	A	B	C	A	B	C	A	B	C
30	17.263	16.363	16.036	6.9147	6.7145	6.4211	5.0521	4.9055	4.6936
110	17.281	16.474	16.490	6.9344	6.8457	6.7824	5.0755	5.0118	4.9643
440	16.926	16.442	16.493	6.8819	6.7983	6.7983	5.0220	4.9643	4.9643
990	16.785	16.468	16.506	6.8819	6.7919	6.8299	4.9996	4.9801	5.0086
1760	16.703	16.474	16.506	6.8448	6.8299	6.7983	4.9996	4.9959	4.9643

III. NUMERICAL RESULTS

The numerical validation of the proposed methodology is performed by means of various orthogonal, partially filled with a material of relative permittivity ε_r, resonator configurations. The resonant cavities, of dimensions $0.2 \times 0.1 \times 0.111$ m^3 which are characterized by a dielectric interface that varies according to function [12]

$$D_I(x) = \frac{b}{2}\left(0.01 + 0.99\exp(-q^2(x/a - 0.5)^2)\right) \quad (8)$$

a and b being the width and the height of the structure, and q a curvature parameter, are excited by a Gaussian in space and time distribution. The frequency domain results are extracted from the implementation of the Fourier transform on the, filtered by a Blackman–Harris window, time samples.

The results derived by the innovative lattice structure are compared with those of two staircase FDTD techniques, the standard and an enhanced one [8].

Specifically, the efficiency of the proposed algorithm is tested for a series of different interface curvatures obtained by varying parameter q, while the filling material remains the same ($\varepsilon_r = 38$). The results are shown in Table I where the fourth resonant frequency of the cavity for three values of q ($q = 1, 2, 3$) is computed. The promising performance of the new scheme is obvious, since even for very coarse meshes, it is significantly accurate. Furthermore, no instabilities are observed as the grid becomes denser despite the large number of time steps that were used so as to examine the limits of the algorithm.

The proposed technique was, also, tested for various values of the filling material permittivity, since a higher dielectric discontinuity is more difficult to be accurately modeled. Nevertheless, as shown in Table II, the new scheme preserves its accuracy, thanks to the precise geometric representation of the interface and the use of the effective permittivity scheme along the interface.

Consequently, the overall computational resources needed for a specific level of accuracy is significantly reduced as proved by the comparative study of Table III, where the CPU time and memory requirements of the three methods and the fourth resonant frequency computed by them for various grids, are listed. This important advantage of the proposed methodology is based on its ability to obtain remarkable precision while simultaneously maintaining in a major level the simple and easy-to-program structure of the standard FDTD algorithm.

TABLE III
COMPARISON OF THE COMPUTATIONAL RESOURCES. CALCULATION OF THE 4th RESONANT FREQUENCY FOR $q = 3$ AND $\varepsilon_r = 38$

No of cross-section cells	Proposed Method			Staircase/[8] Methods		
	CPU time	Memory (MB)	Frequency ($\times 10^8$)	CPU time	Memory (MB)	Frequency ($\times 10^8$)
30	14"	0.066	6.2015	8"	0.046	5.851
110	2' 10"	0.174	6.2156	1' 52"	0.150	6.1026
440	21' 58"	1.30	6.1884	17' 22"	1.07	6.1342
990	1h 25'	4.34	6.166	1h 21'	3.37	6.1184
1760	6h 57'	10.24	6.1435	6h 53'	7.67	6.134

IV. CONCLUSION

A conformal FDTD technique for the modeling of curved dielectric interfaces in three dimensions was presented in this paper. It constitutes a feasible and systematic tool for applications involving nonorthogonal dielectric structures, thanks to a successful combination of prism and hexahedral cells. The performance of the scheme was tested via the numerical analysis of resonant cavities, partially filled with dielectric materials.

REFERENCES

[1] A. Taflove, *Computational Electrodynamics. The Finite-Difference Time-Domain Method*. Boston, MA: Artech House, 1995.

[2] T. Jurgens, A. Taflove, K. Umashankar, and T. G. Moore, "Finite-difference time-domain modeling of curved surfaces," *IEEE Trans. Antennas Propagat.*, vol. 40, pp. 357–365, Apr. 1992.

[3] Y. Hao and C. J. Railton, "Analyzing electromagnetic structures with curved boundaries on Cartesian FDTD meshes," *IEEE Trans. Microwave Theory Tech.*, vol. 46, pp. 82–88, Jan. 1998.

[4] J. Fang and J. Ren, "A locally conformed finite-difference time-domain algorithm of modeling arbitrary shape planar metal strips," *IEEE Trans. Microwave Theory Tech.*, vol. 41, pp. 830–838, May 1993.

[5] N. K. Madsen, "Divergence preserving discrete surface integral methods for Maxwell's curl equations using nonorthogonal unstructured grids," *J. Comp. Phys.*, vol. 119, pp. 34–45, 1995.

[6] C. H. Chan and J. T. Elson, "A vertex-based finite-volume time-domain method for analyzing waveguide discontinuities," *IEEE Microwave Guided Wave Lett.*, vol. 3, pp. 372–374, Oct. 1993.

[7] N. Kaneda, B. Houshmand, and T. Itoh, "FDTD analysis of dielectric resonators with curved surfaces," *IEEE Trans. Microwave Theory Tech.*, vol. 45, pp. 1645–1649, Sept. 1997.

[8] W. Yu and R. Mittra, "A conformal finite difference time domain technique for modeling curved dielectric surfaces," *IEEE Microwave Wireless Comp. Lett.*, vol. 11, pp. 25–27, Jan. 2001.

[9] K.-P. Hwang and A. C. Cangellaris, "Effective permittivities for second-order accurate FDTD equations at dielectric interfaces," *IEEE Microwave Wireless Comp. Lett.*, vol. 11, pp. 158–160, Apr. 2001.

[10] A. Bossavit and L. Kettunen, "Yee-like schemes on staggered cellular grids: A synthesis between FIT and FEM approaches," *IEEE Trans. Magn.*, vol. 36, pp. 861–867, July 2000.

[11] S. D. Gedney and J. A. Roden, "Numerical stability of nonorthogonal FDTD methods," *IEEE Trans. Antennas Propagat.*, vol. 48, pp. 231–239, Feb. 2000.

[12] A. Ioffe and A. Dreher, "Discrete mode matching method for the analysis of quasiplanar structures," in *Proc. IEEE AP-S Int. Symp. URSI Radio Sci. Meet.*, Orlando, FL, July 1999, pp. 1840–1843.